SAE TECHNICAL PAPER SERIES

2002-01-1087

300 kW Switched Reluctance Generator for Hybrid Vehicle Applications

Gabriel Gallegos-Lopez, Fred Reiter, Jr., Kaushik Rajashekara and Ronald J. Krefta
Energenix Center, Delphi Automotive Systems

Reprinted From: Advanced Hybrid Vehicle Powertrain Technology (SP–1697)

The Engineering Society For Advancing Mobility Land Sea Air and Space®
INTERNATIONAL

SAE 2002 World Congress
Detroit, Michigan
March 4-7, 2002

The appearance of this ISSN code at the bottom of this page indicates SAE's consent that copies of the paper may be made for personal or internal use of specific clients. This consent is given on the condition, however, that the copier pay a per article copy fee through the Copyright Clearance Center, Inc. Operations Center, 222 Rosewood Drive, Danvers, MA 01923 for copying beyond that permitted by Sections 107 or 108 of the U.S. Copyright Law. This consent does not extend to other kinds of copying such as copying for general distribution, for advertising or promotional purposes, for creating new collective works, or for resale.

Quantity reprint rates can be obtained from the Customer Sales and Satisfaction Department.

To request permission to reprint a technical paper or permission to use copyrighted SAE publications in other works, contact the SAE Publications Group.



GLOBAL MOBILITY *DATABASE*

All SAE papers, standards, and selected books are abstracted and indexed in the Global Mobility Database

No part of this publication may be reproduced in any form, in an electronic retrieval system or otherwise, without the prior written permission of the publisher.

ISSN 0148-7191
Copyright 2002 Society of Automotive Engineers, Inc.

Positions and opinions advanced in this paper are those of the author(s) and not necessarily those of SAE. The author is solely responsible for the content of the paper. A process is available by which discussions will be printed with the paper if it is published in SAE Transactions. For permission to publish this paper in full or in part, contact the SAE Publications Group.

Persons wishing to submit papers to be considered for presentation or publication through SAE should send the manuscript or a 300 word abstract of a proposed manuscript to: Secretary, Engineering Meetings Board, SAE.

Printed in USA

2002-01-1087

300 kW Switched Reluctance Generator for Hybrid Vehicle Applications

Gabriel Gallegos-Lopez, Fred Reiter, Jr., Kaushik Rajashekara and Ronald J. Krefta
Energenix Center, Delphi Automotive Systems

Copyright © 2002 Society of Automotive Engineers, Inc.

ABSTRACT

The switched reluctance generator, because of its simple and robust structure, is attractive as an auxiliary power unit (APU) in lightweight, high-speed and high power military, and other types of vehicles. In this paper, investigation and design analysis of a 300 kW switched reluctance generator is presented. Five different designs of the machine are evaluated to provide 300 kW at 30,000 rpm, 60,000 rpm, and at 100,000 rpm. The different designs are compared in terms of size, weight, efficiency, and torque. Analyses of the mechanical stress and critical speeds are also presented. Recommendations are presented for the selection of the best design methodology for APU application in Hybrid vehicles.

INTRODUCTION

Switched reluctance generators (SRG), due to their simple construction, fault tolerance and robustness, are gaining importance in a wide range of applications. Recently there has been significant research in SRG's [1, 2].

The SRG is a doubly salient machine. It does not have any magnets or brushes, and the phases are completely independent. The rotor is made of laminated iron and it does not have any windings. This makes the SRG mechanically robust, and therefore, suitable for high speed applications [3]. Furthermore, the SRG has a high torque/inertia ratio, and high efficiency.

In this paper, the use of switched reluctance generator as an auxiliary power unit in high power hybrid vehicle applications is investigated. Five different designs of the machine are evaluated to provide 300 kW at 30,000 rpm, 60,000 rpm, 100,000 rpm, and 100 kW at 100,000 rpm. The trends of variables such as size, weight, efficiency, and torque for each design are presented. Analyses of the mechanical stress and critical speeds are also presented. The detailed design and performance of each machine are discussed in the following sections.

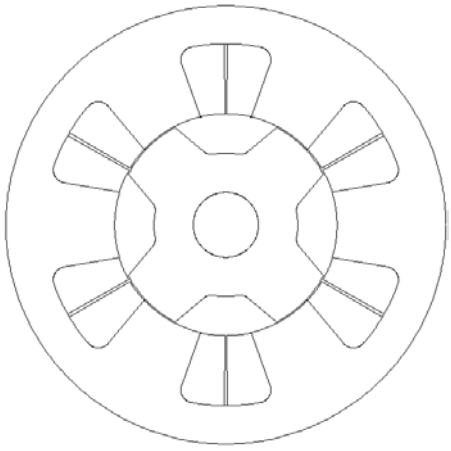


Figure 1. 6/4 3-phase SRG cross section.

The paper discusses the key factors of machine design, and five designs are proposed. Rotor dynamic analysis, and material characteristics are also discussed. This is followed by the electrical simulation of each machine design, and the trade off's of the different designs are discussed. Finally, recommendations are presented for the best design.

MACHINE DESIGN

In order to keep a good balance between robustness and total power device cost, the machine topology that is chosen is the 6 stator pole, 4 rotor pole 3-phase. This topology can provide 2/3's of the rated power in case one of the phases fails. Another factor that needs to be considered for high-speed applications is the core losses, which are proportional to the square of the number of strokes per revolution. The 6/4 3-phase SRG has 12 strokes per revolution, which is half the number of strokes of the 8/6 4-phase SRG. Therefore, the 6/4 3-phase machine was chosen. It offers a good balance between robustness and number of strokes per revolution. A typical 6/4 3-phase machine cross section is shown in Fig. 1. Designs of the following SRG's were carried out using the 6/4 3-phase SRG topology:

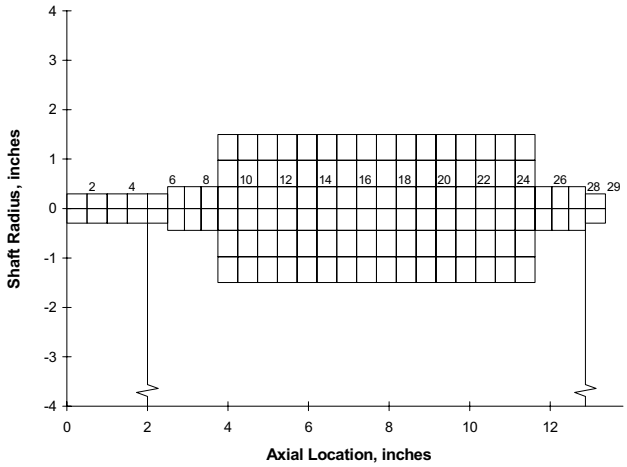


Figure 2. Mechanical model of the 300 kW, 100,000 rpm SRG rotor.

1. SRG I: 300 kW @ 100,000 rpm,

2. SRG II: 300 kW @ 60,000 rpm,

3. SRG III: 300 kW @ 30,000 rpm (small diameter-long stack length),

4. SRG IV: 300 kW @ 30,000 rpm (large diameter-short stack length),

5. SRG V: 100 kW @ 100,000 rpm.

ROTOR DYNAMIC ANALYSIS

The rotor structure along with the bearings and housing form a spring-mass-damper system that is excited by the rotating imbalance which remains after the rotor balancing operation is completed. The rotating imbalance produces a per revolution input force such that when the rotor speed/frequency equals a rotor assembly natural frequency/critical speed a resonant mode results. Without damping, resonant modes can bring about rotor or bearing failure. Typical high speed, machine design methods are to either design the machine so that it does not have any resonant modes/critical speeds in the operating range or to provide sufficient damping so that the resulting vibrations prove non-destructive [4]. Rotordynamic analyses are performed to determine operating speeds at which the motor goes into mechanical resonant modes that are potentially destructive. With the aid of rotordynamic analyses rotors, bearings and housings can be designed to eliminate or mitigate the effects of mechanical resonant modes.

An important design variable is the rotor radius. It is important because radial and tangential stresses are proportional to the square of the radius and to the rotor speed, ($\sigma \sim r^2 * \omega$) [5]. To avoid overstressing the rotor at high speeds, it is desirable to design the rotor radius as small as possible.

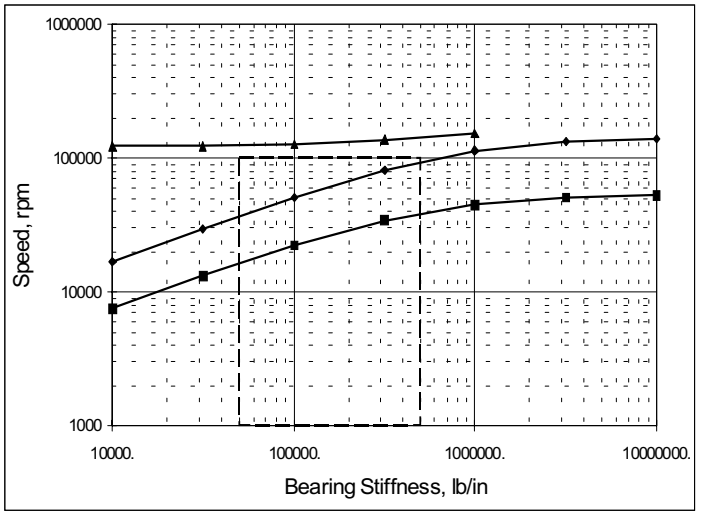


Figure 3. Undamped Critical Speed Map.

However, since machine output power is proportional to the radius squared times the stack length ($P \sim r^2 * L_{stk}$), designing with a smaller than necessary radius requires a longer stack length, which can lead to excessive bearing span, shaft flexure and potentially destructive vibrations.

A rotordynamic (critical speed) analysis has been performed for SRG I using the XLRotor program [6]. An axisymmetric geometry plot of the model is shown in Fig. 2, in which the two bearings are modeled as springs at stations 5 and 28 respectively.

The following assumptions are considered:

1. The rotor teeth regions are modeled as solid axisymmetric elements with reduced mass densities. The real materials are not axisymmetric nor do they occupy 100% of the space assigned to the region. The real materials will be less stiff since they do not occupy 100% of the region and are not “solid” like the program calculates them.

2. This is a rotor model only. It does not include the stiffness of the housing or the mounting. If the housing and mounting are solid and sufficiently stiff no significant changes in critical speeds are to be expected.

The Undamped Critical Speed Map, shown in Fig. 3., is normally used early in the design process as an indicator, as to determine whether critical speeds are liable to occur in the operating range. This is determined using the knowledge: 1) that typical ball bearing spring stiffness is in the range of 50,000 lbs/in to 500,000 lbs/in (90-900 kN/cm), 2) that critical speeds result from exciting a natural frequency within the rotor assembly at a rate of once per revolution due to the small rotating imbalance that remains after balancing. The curves displayed in Fig. 3. represent motor resonant modes. Determining whether natural frequencies/resonant modes occur in the region of interest (shown in the dashed rectangle in Fig. 3), will help guide the bearing/damping details of the further design.

Table 1. Spring constant and damping coefficients.

	Spring constant [lb/in]			SFD
Rotational speed [rpm]	Squeeze film Damper	Ball bearing	Total	Damping coefficient [lb_f-sec/in]
100	113	347,314	112	68.7
10,000	11,254	341,839	10,895	68.7
20,000	173,109	293,506	108,887	69.1
22,169	350,990	241,447	143,046	69.9
30,000	205,489	242,750	111,285	68.9
40,000	160,768	176,575	84,151	68.8
50,000	151,029	127,340	69,088	68.7
60,000	142,130	100,190	58,765	68.7
70,000	102,092	83,182	45,836	68.7
80,000	36,616	73,546	24,445	68.7
90,000	8,202	68,704	7,327	68.7
100,000	40,952	68,237	25,593	68.7
110,000	135,340	68,412	45,442	68.7
120,000	147,643	70,122	47,542	68.7

As can be seen there are 2 curves in the operating speed region (0 to100,000 rpm). It can be noted that the two curves increase in speed as the stiffness increases which is in accordance the natural frequency equation, $\omega_n = (k/m)^{1/2}$, where k is the stiffness and m is the mass of the rotor assembly. Because two natural frequencies do occur within the operating region it is necessary to include dampers in conjunction with the bearings to prevent excessive vibrations at critical speeds from destroying the bearings.

Bearing input information (spring constants) along with damper input is shown in Table 1. Typical ball bearings consistently lose spring tension as the speed increases which is a result of centrifugal forces on the balls leading to increased outer race loading and decreased inner race loading which allow the balls to skid against the inner race and change the contact angle [7]. The spring constants of squeeze film dampers are low when the load is low and high when the load is high. When ball bearings and squeeze film dampers are placed in series the combination of the two provides an overall lower spring constant in accordance with the equation, $k_t = 1/(1/k_s + 1/k_d)$ where k_t, k_s and k_d are the overall spring constant, the bearing spring constant and the damper spring constants respectively.

The lower overall spring constant resulting from combining the ball bearings with squeeze film dampers changes the critical speeds. Instead of two critical speeds in the operating range the rotordynamic analysis indicates SRG I has a critical speed at 22,169 rpm as shown in Fig. 4. This is the speed at which the rotor assembly's fundamental bending mode of 22,169 cycles per minute (369 Hz) is excited by the rotating imbalance.

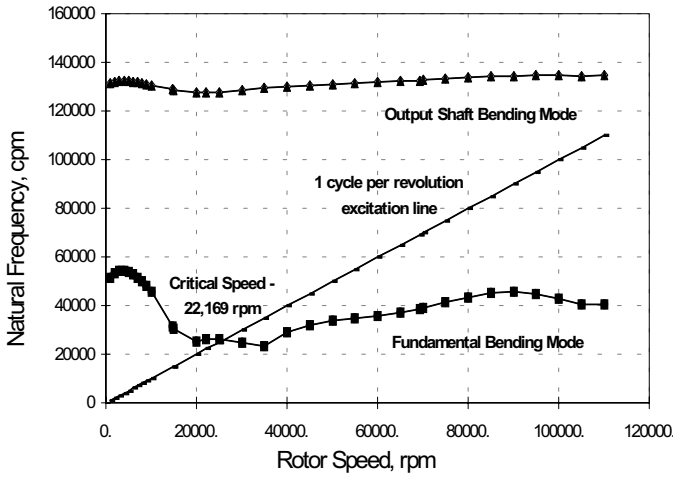


Figure 4. SRG I critical speed at 22,169 rpm.

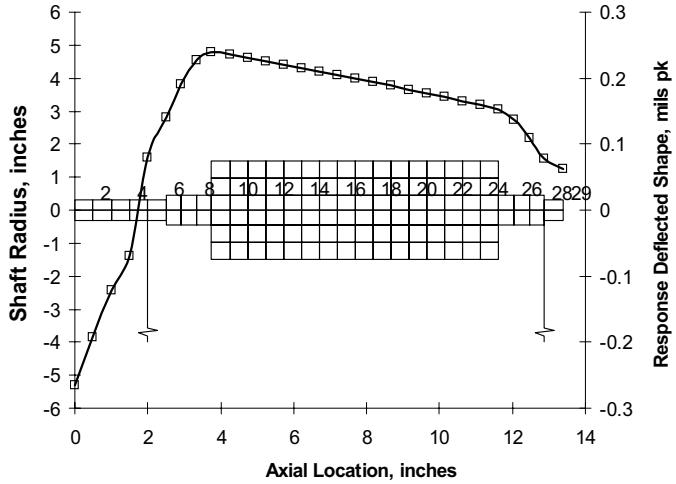


Figure 5. 2-D representation of first bending mode.

Also shown in Fig. 4, the rotor output shaft can be projected to go into resonance well above the 100,000 rpm upper limit of the operating range.

A two dimensional representation of the first bending mode is shown in Fig. 5. As can be ascertained the deflection is acceptably low (< 0.0003" / 0.0076 mm at the most). This is the result of a high precision balance specification and the squeeze film dampers that limit the vibration and allow both safe operation at the first bending mode while moving the second resonant mode out of the operating range. The rotor is balanced to an exacting 4.2 gm-mm i.e. an imbalance of 4.2 gm, 1 mm from the central axis of a rotor that weighs 5.43 kg. The level of vibration displayed in Fig. 5 is the result of the imbalance as it is applied at stations 9 and 25 (ends of the rotor laminations). The bearings chosen for this application are angular contact ball bearings with an oil mist lubrication system. Bearing ball contact loads, stresses and deflections have been calculated for all speeds and are within acceptable ranges. The squeeze film damper (SFD) consists of a metered oil flow trapped between the bearing's outer race, two O-rings and an outer SFD ring.

Table 2. Mechanical stress.

	SRG I, V 100 krpm AISI 4340 R-OD = 76mm		SRG II 60 krpm AISI 4130 R-OD = 76mm		SRG III, IV 30 krpm AISI M-15 R-OD = 136.8mm	
Stress	Max.	Avg.	Max.	Avg.	Max.	Avg.
Rad. [kpsi]	249.7	62.2	57.3	19.5	36.1	14.8
[MPa]	1722	429	395	134	249	102
Tang. [kpsi]	200.6	148.0	71.5	51.5	57.2	40.9
[MPa]	1383	1020	493	355	394	282

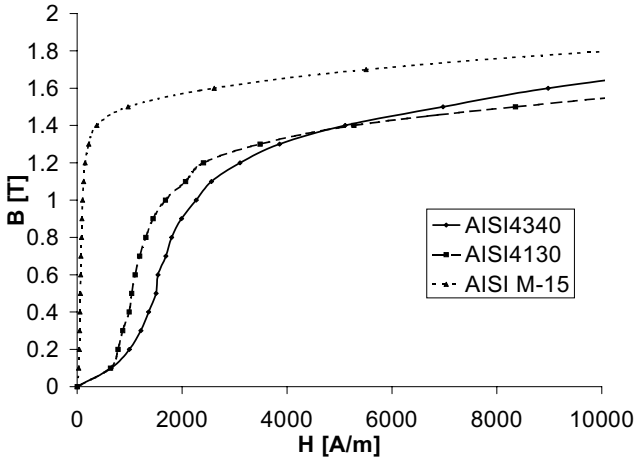


Figure 6. B-H curves for AISI 4340, 4130 and M-15.

The radial clearance between bearing outer race and SFD outer ring is 0.0018" (0.0046 mm). A typical operating pressure is 20 psi (138 kPa).

Based on stress values obtained from closed form solutions and the strengths of rotor steels, operating at 100,000 rpm, the maximum allowable rotor diameter is 76 mm. Hence, the following rotor diameters are selected: 76 mm (SRG's I-III & V), and 136.8 mm (SRG IV). The selected steels are AISI 4340 (SRG's I & V), AISI 4130 (SRG II) and AISI M-15 (SRG's III & IV).

Table 2 summarizes the maximum and average radial and tangential stresses. The yield strength for the selected steels is as follows. AISI 4340 is the strongest with 243,000 psi (1675 MPa), then AISI 4130 follows at 103,000 psi (710 MPa) and AISI M-15 has a 71,000 psi (490 MPa) yield limit. Note that for SRG's I and V the maximum stress is close to the maximum material strength.

MATERIAL MAGNETIC CHARACTERISTICS

The magnetic characteristics (B-H curve) for the different steels are plotted in Fig. 6. AISI M-15, in dotted line, gives the largest slope close to 0 A/m. Its curve increases linearly very close to the B-axis. Note that its magnetic saturation starts around 1.4 T.

Table 3. Dimensions of the five SRG designs.

	SRG I	SRG II	SRG III	SRG IV	SRG V
Phases	3	3	3	3	3
Stator poles	6	6	6	6	6
Rotor poles	4	4	4	4	4
S-OD [mm]	152	152	152	273.6	152
R-OD [mm]	76	76	76	136.8	76
Shaft dia. [mm]	22.52	22.52	22.52	40.54	22.52
Airgap [mm]	0.4	0.4	0.4	0.4	0.4
Stack length [mm]	200	250	370	165	76
Stator pole arc [^{o} mech.]	34	34	34	34	34
Rotor pole arc [^{o} mech.]	35	35	35	35	35
Steel	AISI 4340	AISI 4130	AISI M-15	AISI M-15	AISI 4340
Turns/phase	5	7	8	10	14
Slot area [mm^2]	621.5	621.5	621.5	2051.6	621.5
Slot fill	0.35	0.35	0.35	0.35	0.35
Voltage [V]	600	600	600	600	600
Max. Ind. [μH]	85	243	828	984	256
Min. Ind. [μH]	15	37	69	56	54
Saliency ratio	5.7	6.6	12	17.6	4.7
Rated speed [krpm]	100	60	30	30	100
Rated power [kW]	300	300	300	300	100
Current density [A/mm^2]	13.3	16.5	17.1	5.8	13.1

This indicates that M-15 steel has good magnetic properties. In contrast, AISI 4130, in dashed line, and AISI 4340, in solid line, curves rise with much smaller slope than AISI M-15, with AISI 4340 having the smallest slope. The magnetic saturation for both AISI 4130 and AISI 4340 starts at 1.2 T. It is important to mention that around before 5,000 A/m AISI 4130 has greater permeability than AISI 4340. However, above 5,000 A/m AISI 4340 has greater permeability, reaching 2.2 T around 46,000 A/m. AISI M-15, and AISI 4130 reach 2.2 T at 77,500 A/m and 149,800 A/m respectively. It is worth noting that the hysteresis band in the B-H curve for AISI 4340 (not plotted here), which is proportional to the core losses, is the largest, followed by the AISI 4130. AISI M-15 has the smallest hysteresis band.

Summarizing the properties of the selected steels, starting from the highest strength, the order is AISI 4340, AISI 4130 and AISI M-15. In contrast, starting with the steel with better magnetic characteristics the opposite order exists. Hence, there is a trade off between high strength steel and steel that has good magnetic properties. At high speed, such as 100,000 rpm, there is no choice but to use the strongest steel available. Starting from the rotor outer diameter, the rest of the machine dimensions were obtained based on hand calculation and simulations. Table 3 summarizes the characteristics of the five machine designs under investigation.

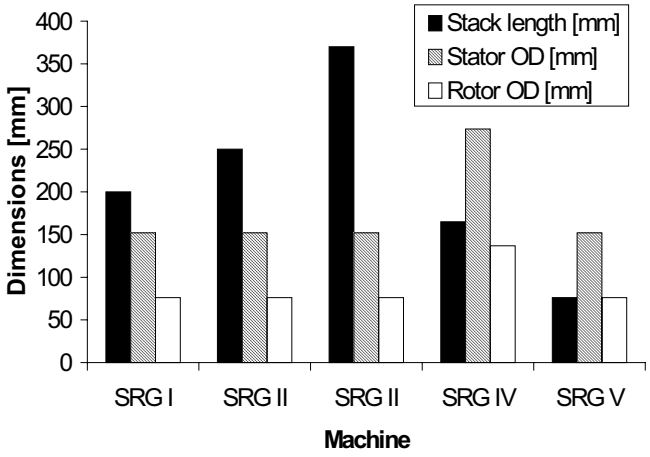


Figure 7. Stack length, S-OD and R-OD for each design.

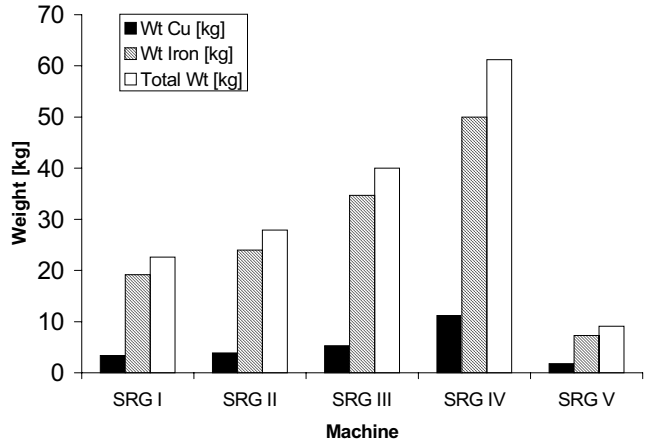


Figure 8. Copper weight, iron weight and total weight for each design.

SIMULATION RESULTS

The performance of the different designs was investigated using PC-SRD program [8]. The design variables such as rotor diameter, stack length and number of turns per pole were adjusted in order to obtain rated power at given rated speed. The steel was also changed where it was possible in order to obtain better machine performance.

Fig. 7 shows the stack length, the stator outer diameter (S-OD) and the rotor outer diameter (R-OD). The R-OD was designed to be half the S-OD. Note that if the S-OD is kept fixed, the stack length is inversely proportional to the rated speed of the machine for the same power. The stack length to R-OD ratios for the different designs are 2.6, 3.3, 4.9, 0.8 and 1 for SRG I, II, III, IV and V respectively. The ratio of SRG III is excessive at approximately 5; this design is at risk of a resonant failure. Therefore, a second machine (SRG IV) was designed for operation at 300 kW @ 30,000 rpm. In this design the R-OD is increased by a factor of 1.8.

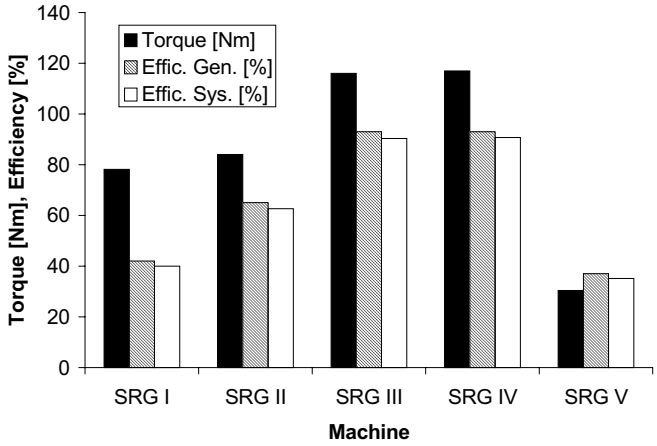


Figure 9. Torque and efficiency for each design.

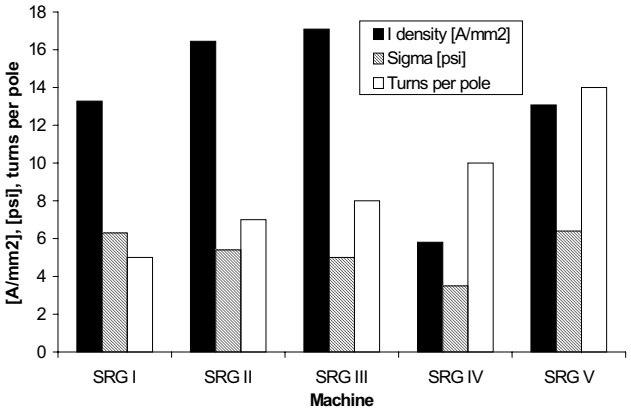


Figure 10. Current density, airgap shear stress and turns per pole for each design.

Consequently, the stack length is reduced from 370 mm to 165 mm yielding a more reasonable stack length-to-diameter ratio of 0.8.

The copper weight, the iron weight, and total weight are shown in Fig. 8. This figure shows that for the same generated power the machine tends to be heavier as the rated speed is reduced. Note that SRG IV is heavier than SRG III. The reason is that the volume increases with the square of the stator diameter. Comparing SRG V and I, it is found that SRG V is approximately half the weight of SRG I. However, it generates only 1/3 of the power of SRG I.

The torque and efficiency for each design are depicted in Fig. 9. The relation of Power = Torque X Speed is observed here. Note that the generator efficiency and the system efficiency are very similar due to high efficiency in the power converter (around 95% for all cases). It is also observed that the generator efficiency is inversely proportional to the speed. The maximum efficiency is obtained with SRG's III and IV. Note that the core losses are less in these designs compared with the other designs because better magnetic steel (AISI M-15) can be used, and their based speeds are significantly less.

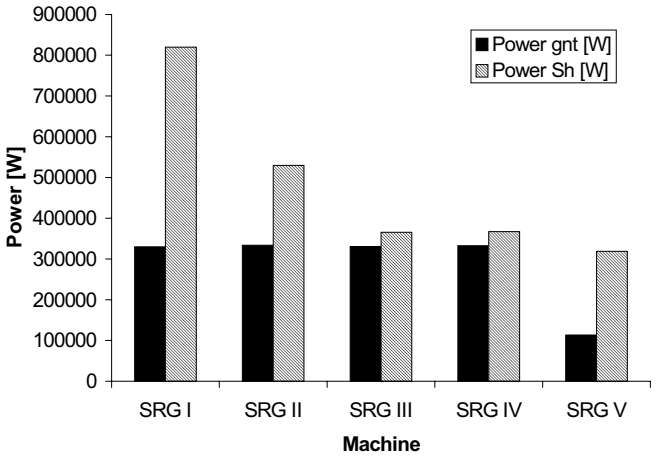


Figure 11. Generated and shaft power for each design.

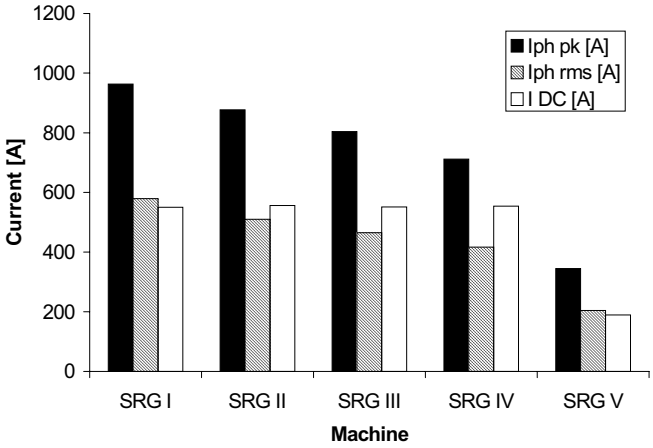


Figure 12. Peak phase current, rms phase current and generated DC current for each design.

The windage losses are also less at 30,000 rpm. Comparing SRG I and V, it can be observed that their efficiencies are comparable while the torque of SRG V is approximately 1/3 of the torque of SRG I.

Fig. 10 depicts the current density, the airgap shear stress (sigma) and the number of turns per pole for each design. SRG III has the maximum current density of approximately 17 A/mm^2. SRG II has slightly less current density at 16.5 A/mm^2. The current density of SRG I is less than the previous two at 13.3 A/mm^2. Observe that the difference in current density between SRG III and IV is significant. SRG IV has less current density than SRG III. The reason is that SRG IV has larger copper area due to its larger S-OD. Note that while SRG's I, II, III and V may need to be liquid or oil cooled due to their large current densities, SRG IV can be air cooled because of its low current density around 5.8 A/mm^2. Despite the fact that SRG V produces 1/3 of the power of SRG I, the current density of both are similar because SRG V has 2.8 times the number of turns of SRG I for the same copper area.

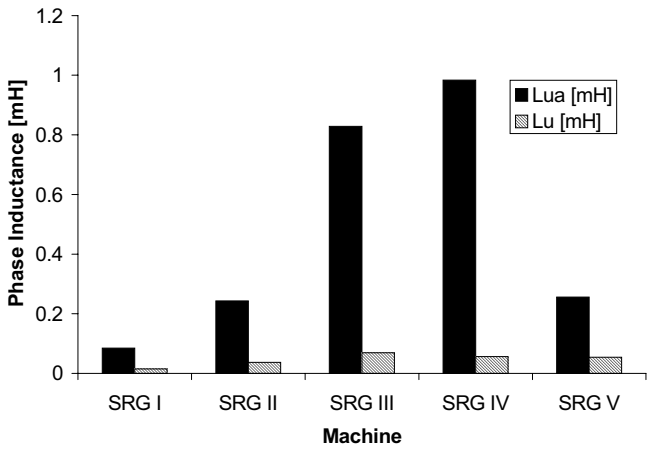


Figure 13. Phase inductance for each design.

SRG's I and V have very similar airgap shear stress (sigma) around 6.4 psi, which is the largest and most volume efficient of the designs. Note that SRG IV has the lowest airgap shear stress due to its lower operating speed combined with a large volume. The number of turns is inversely proportional to the speed. This is because for a given voltage in the DC-link, the machine is more voltage limited as the speed is increased. Hence, the phase inductance has to be small in order to be able to excite the machine.

Fig. 11 depicts the generated electrical power and mechanical shaft power. It is clear that while the generated power is constant for SRG I, II, III and IV, the required shaft power varies significantly for each machine. The difference between them is the system power loss. It is observed that the power loss is substantial in SRG I. The reason is that the steel AISI 4340 is poor magnetically and has large core losses. The other important source of losses is the windage losses, which is large at 100,000 rpm. SRG II has less system loss because of better magnetic material and less base speed. For the cases of SRG's III and IV, the generated power and shaft power are basically the same. It is worthy noting that the losses in these two machines are relatively small. The improvement is because much better steel (AISI M-15) can be used at 30,000 rpm. SRG V presents large losses due to core and windage losses.

Fig. 12 depicts the peak phase current, the rms phase current and the generated DC current. It can be observed that SRG I has the highest peak current, which is close to 1000 A. Note that the peak current is proportional to the speed. The peak current for SRG II, III and IV is around 900 A, 800 A and 700 A respectively. Likewise, the rms phase current follows the same trend as the peak current. The rms current for SRG I, II, III and IV are 580 A, 510 A, 465 A and 417 A respectively. In contrast, the generated current is constant around 550 A for each design. It is worth noting that the generated DC current and the rms current are very similar for SRG V, at approximately 200 A while the peak current is 345 A.

The unsaturated aligned phase inductance (Lua) and the unaligned phase inductance (Lu) are depicted in Fig. 13. It can be observed that both inductances are inversely proportional to the speed. The machine SRG I with maximum speed has the minimum phase inductance. It is important to note that despite the fact these inductances are small they do not put a constraint in the power switches. The reason is that the SRG is operated in single pulse. Therefore, it does not need current regulation. The switching frequency of the power devices is the commutation frequency.

An important factor in the SRG design is the ratio Lua/Lu. SRG's I, II, III, IV and V have a Lua/Lu ratio of 5.7, 6.6, 12.0, 17.6 and 4.7 respectively. Note that SRG's III and IV have significant larger Lua/Lu ratio than the rest of the designs due to the use of good magnetic material for these designs. To maximize the torque per ampere of the machine and decrease the size of the power converter, a Lua/Lu ratio as large as possible is desired.

CONCLUSIONS

Designs for five different switched reluctance generators have been investigated to obtain the trends of important variables such as size, weight, efficiency and torque. The 6/4 3-phase SRG topology was chosen for this high-speed/high-power application because it offers good balance between robustness and core losses. For very high speed operation such as 60,000 rpm and 100,000 rpm there is no choice but to use high strength steels that are able to support the mechanical stresses (AISI 4340 and AISI 4130 respectively) rather than to use a steel with good magnetic properties. In contrast, for a 30,000 rpm design, better magnetic steel (AISI M-15) can be utilized because the mechanical stress is significantly less than at 100,000 rpm and 60,000 rpm.

It was found that machines with a lower rated speed are heavier for a given generated power. Machines with very high operating speeds tend to be long because the centrifugal forces limit the R-OD. The rotordynamic implications of a long stack length lead to more complicated and costly bearing lubrication systems employing oil mist bearings and squeeze film dampers. High-speed machines also tend to have poor efficiency because the core losses and windage losses are large. They tend to have high current density because the slot depth/copper wire area is more limited on small diameter-high speed than on large diameter-low speed machines. It should be noted that SRG IV with its low current density is the only machine that can be air-cooled. The other four designs will require liquid or oil cooling and significantly more expensive coolant systems. On the other hand, the number of turns per pole and phase inductance are inversely proportional to rated speed. Lower turns per pole are desired in order to have small phase inductance and be able to sufficiently excite the generator.

Table 4. Critical parameters for APU decision making.

	S-OD [mm]	Stack length [mm]	Total weight [kg]	Current density [A/mm^2]	Sys. effic. [%]	Input power [kW]
SRG I	152	200	22.6	13.3	40.0	820
SRG II	152	250	27.9	16.5	62.7	530
SRG III	152	370	40	17.1	90.4	366
SRG IV	273.6	165	61.2	5.8	90.8	367
SRG V	152	76	9.1	13.1	35.2	319

Machines at high speed tend to have a small Lua/Lu ratio due to the poor magnetic properties of the steel. This leads to lower efficiencies.

Table 4 summarizes the main critical parameters that are necessary to decide which is the most appropriate design to utilize for a high power, high speed APU. The final conclusion on which design to choose has to be based on which set of criterion are valued most. If high efficiency and low cost are valued more highly than size and weight then SRG IV (300 kW @ 30,000 rpm) is the best choice. If electric machine size and weight are of most concern then SRG I (300 kW @ 100,000 rpm) is the best choice. Caution, however, should be used in choosing SRG I since the efficiency is low, thereby requiring the prime mover to be 870 kW, which will likely make the prime mover larger and heavier as well as requiring a large fuel supply to power it. It should be noted that SRG IV is close to the state-of-the-art and therefore feasible.

ACKNOWLEDGMENTS

This project was partially funded by Defense Advance Research Project Agency (DARPA).

CONTACT

Gabriel Gallegos-Lopez, Delphi Automotive Systems, Energenix Center, M/C D35, P.O. Box 9005, Kokomo, IN, 46904-9005, USA.
E-mail: gabriel.gallegos@delphiauto.com

REFERENCES

1. E. Richter, and C. Ferreira. IEEE Proc. IAS'95, pp. 434-440, 1995.
2. A. V. Radun, C. A. Ferreira, E. Richter. IEEE Trans. IA, 34(5):1026-1034, 1998.
3. C. M. Stephens. IEEE Trans. IA, 27(6):1098-1102, 1991.
4. Robert Zeillinger, and Hubert Kottritsch, "Damping in a Rolling Bearing Arrangement", Evolution, Jan., 1996.
5. TJE Miller, Switched reluctance motors and their control. Magna Physics Pub., Clarendon Press, Oxford, 1993.
6. Rotordynamic software by Rotating Machine Analysis, Inc.,7701 Baja Cove, Austin, TX 78759.
7. Leif Lewinschal, "Bearings for High Speed Operations", Evolution, Feb., 1994.
8. TJE Miller. PC-SRD 6.9 software, Glasgow University, 1995.